MODELLING THE LOW VELOCITY IMPACT RESPONSE OF AN AEROSPACE COMPOSITE REPLACEMENT PANEL

Javid Bayandor*, Rodney S. Thomson, Paul J. Callus*****
The Sir Lawrence Wackett Aerospace Centre
School of Aerospace, Mechanical and Manufacturing Engineering
Royal Melbourne Institute of Technology
****Cooperative Research Centre for Advanced Composite Structures***
*****Air Vehicles Division, Defence Science and Technology Organisation***

Keywords: *Composite Replacement Panel Technology, Damage Tolerance, Low Velocity Impact, Delamination*

Abstract

This paper reports the results of an investigation of the damage generated by low velocity impact in a composite laminate. The laminate represented the mid-bay skin of a Composite Replacement Panel (CRP) demonstrator. Coupon level test specimens were damaged using a drop-weight impactor with an instrumented tup. The resulting damage was characterised using ultrasonic C-Scan. Simulations of these tests were run on finite element models of the coupons. The area of delamination and the force-time history for the impact event were predicted using the fabric bi-phase material model and Crisfield delamination criterion implemented in the explicit finite element code Pam-Crash. Good agreement was obtained between the simulation and tests results. This analysis technique shall be developed further and used in the airworthiness certification of CRPs and to develop CRPs with enhanced resistance to low velocity impact.

1. Background

1.1 General

As with most defence forces, budgetary limitations and high replacement costs mean that the Australian Defence Force (ADF) must extend the economic life of its aircraft. One of the high cost items in managing aircraft is the requirement to maintain structure that has been damaged or deteriorated beyond normal repair limits. This is typically done by purchasing standard replacement parts from the Original Equipment Manufacturer (OEM). This approach becomes increasingly difficult as the aircraft fleets age. In some cases, the OEM may even cease to exist. An attractive alternative for the ADF is to develop and maintain an Australian capability to support these aircraft.

1.2 Composite Replacement Panel Technology (CRPT)

As one aspect of such a program, the ADF is sponsoring development of Composite Replacement Panel Technology (CRPT). The CRPT will offer the capability to replace metallic structure, particularly metallic bonded panels, with structure that has been manufactured from advanced fibre composites [1]. It is being developed by the Defence Science and Technology Organisation (DSTO) in collaboration with the Cooperative Research Centre for Advanced Composite Structures (CRC-ACS).

A CRP demonstrator has been produced. Known as Panel I it was designed as a replacement for F-111 Panel 3208 as shown in Fig. 1. The as-manufactured panel is shown in Fig. 2. It was a 870 *mm* wide x 1180 *mm* long

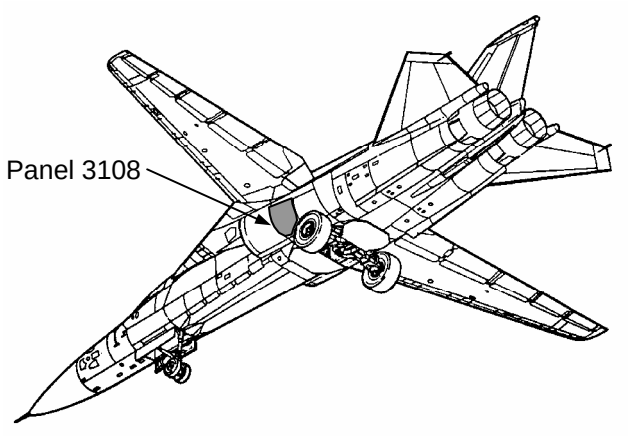

Figure 1: The location of Panel 3108. Panel 3208 is at the same position on the opposite side of the aircraft

Figure 2: The as-manufactured Panel I

skin, stiffened by 12 top-hat stiffeners and an intersecting z-stiffener. Panel I was manufactured from Advanced Composites Group MTM49-3 prepreg, a 200 $g\ m^{-2}$, 2 x 2 twill fabric that was oven cured under vacuum followed by a free standing post-cure. The skin lay-up was $[45_2\ 0\ 45_3\ 0\ 45_3\ 0\ 45_2]$, with $[45]_4$ hat caps and $[45]_3$ hat webs. A static analysis has been conducted on Panel I [2] and a full-scale test of this panel shall be conducted in June 2004.

1.3 The Effect of Low Velocity Impact on Polymer Matrix Composites (PMCs)

PMC aircraft components, including CRPs, do not suffer from the corrosion damage and fatigue cracking that limits the life of their metallic counterparts. However, PMCs are susceptible to impact damage. The most common sources of impact are dropped tools during maintenance, runway debris thrown up during landing and take-off, and hailstones.

Susceptibility to impact arises from the brittle behaviour of fibres and the relatively low stiffness and strength of the matrix resins, coupled with; stiffness mismatches between adjacent plies of different orientations, stress concentrations at fibre-resin interfaces, high inter-laminar shear stresses and large local deformations. Impacts cause delamination, fibre breakage and fibre-resin disbonding. These features are distributed irregularly throughout the region that has been impacted and they can reduce severely the residual strength of the structure [3,4]. The damage features interact with the structure in a complex, non-linear, manner [5]. Effective modelling of these features requires an intricate, non-linear, approach [6,7].

As part of the airworthiness certification of the CRPT it will be necessary to demonstrate the response of CRPs to possible impact events. This may be achieved by either testing each of these impact scenarios or by developing a validated capability to predict the response of CRPs to impact. The latter is preferred due to the substantially lower costs. A validated modelling approach could also be used to design CRPs with improved impact resistance.

This paper reports the results of a numerical and experimental investigation for one likely impact scenario, a low velocity impact to the mid-bay skin of a CRP.

2. Experimental Techniques

2.1 Impact Testing

Coupon level testing was conducted using a variation of the SACMA SRM 3R compression-after-impact (CAI) test method. The flat laminate test specimen was chosen because of experimental and analytical simplicity. It was also expected to simulate the behaviour of mid-bay skins in CRPs. A different specimen geometry would be required to evaluate behaviour of the skin under the stiffeners.

Fourteen 150 *mm* long x 100 *mm* wide CAI specimens were manufactured from a MTM49-3 panel with a $[0_2\ 45\ 0_2]_S$ lay-up. Curing was conducted in accordance with manufacturers specifications. This lay-up was rotated by 45°, in comparison with the skin lay-up of Panel I, in order to reduce material wastage. Additional validation will be required before the modelling presented in this paper could be applied directly to Panel I.

The CAI specimens were impacted using the instrumented drop-weight impactor shown in Fig. 3. The total mass of the impactor was 1.02 *kg*. Coupons were held to the base using the four clamps shown in Fig. 3. The experimental program used two hemispherical impacting tups, 12.5 *mm* diameter and 25.0 *mm* diameter, and seven incident kinetic energies ranging between 1.0 and 15.0 *J*. These energies were achieved by adjusting the height of impactor drop. A single specimen only was impacted with each tup and energy.

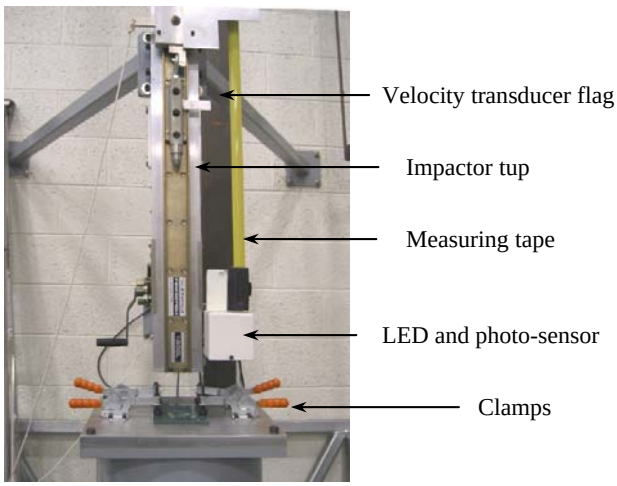

Figure 3: Instrumented drop-weight impact test rig

A four-channel, 100 *kHz*, data acquisition system recorded the force, time, incident velocity and rebound velocity during the impacts.

Time-of-flight ultrasonic C-Scan inspections were conducted on each specimen before and after impacting. The C-Scans showed any manufacturing flaws and the size of delaminations caused by the impact.

2.2 Finite Element (FE) Modelling

Two different types of models were created and analysed during the numerical investigations using the explicit FE code, Pam-Crash V2003 2G. The first model consisted of only the fabric bi-phase material model to enable the study of total damage response of the specimens [8]. The second type of model incorporated both the fabric bi-phase and Crisfield delamination criterion through the use of tied elements and contact interfacial surfaces, the combination of which would allow the prediction of delamination region under the impact zone. Fine grid FE models of the same lay-up and material properties as the CAI coupons were created using MSC.Patran [7].

Schematics of the impactor and the mesh used are illustrated in Fig. 4.

In the first model, the required failure criteria were embedded into the FE models through multi-layered shell elements that used the Pam-Crash fabric bi-phase composite degradation module. Each ply of the laminate was assigned information regarding the fibre (fabric) orientation, anisotropic elasticity, stiffness, strength and damage progression [8]. This approach provided a computationally efficient methodology although it lacked delamination functionality.

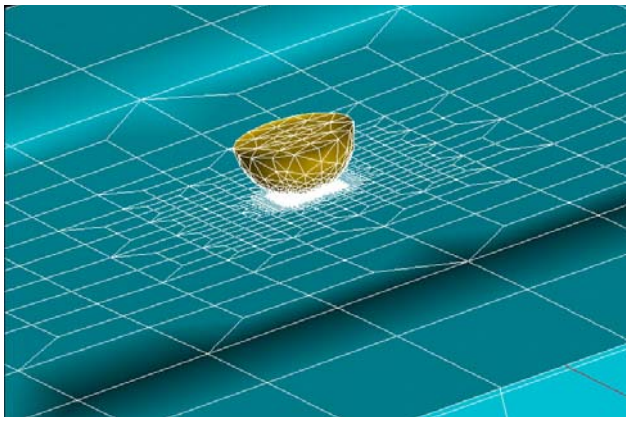

Figure 4: Selected fine mesh region for impact zone

To activate the delamination features in the second model, a combination of six master-slave contact surfaces were implemented into the simulation model. These interfaces modelled the contact between the impactor and the panel as well as between the plies where delamination was expected. Two contact interfaces, denoted by "*d*", were placed between the plies with dissimilar orientations: [0_2 45 *d* 0_4 45 *d* 0_2].

The top ply of the panel on the impact side was defined as the master surface and the impactor was defined as the slave. All other inter-ply contacts were modelled alternately, with the direction of their normals consistent with the impact direction.

The Crisfield delamination criterion used was an adaptation of the tied slide line concept in earlier Pam-Shock versions, where nodes were tied to elements and the contact interfaces were breakable under certain predefined conditions. Previously, this algorithm simply used a penalty approach to create fictitious forces that held slave nodes and segments together. In the recent revision of the code, this approach was extended to include new failure criteria for stiffness as well as Mode I and Mode II rupture. It can further account for the coupling between these failure modes through an interaction criterion [9].

3. Results and Discussion

3.1 Impact Testing

Figures 5 shows the resultant force-time history plots. For impact energies from 1.0 to 7.5 *J* the shape of the force-time plots were quite similar, with the peak force and contact duration rising with impact energy. From 10.0 to 15.0 *J*, as energy increased the peak force decreased slightly while the contact duration increased. This was attributed to the vibration modes between the panel and the impactor as well as the effects of the damage formation.

The C-Scans showed that the as-manufactured CAI specimens were defect free and the impacts generated circular delaminations. A typical C-Scan image is shown in Fig. 6 and the results summarised in Fig. 7.

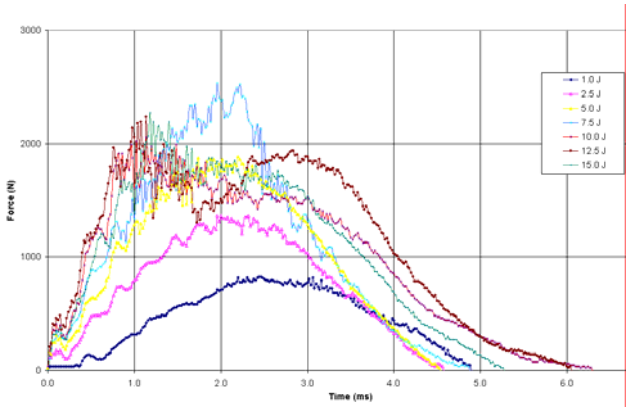

(*a*)

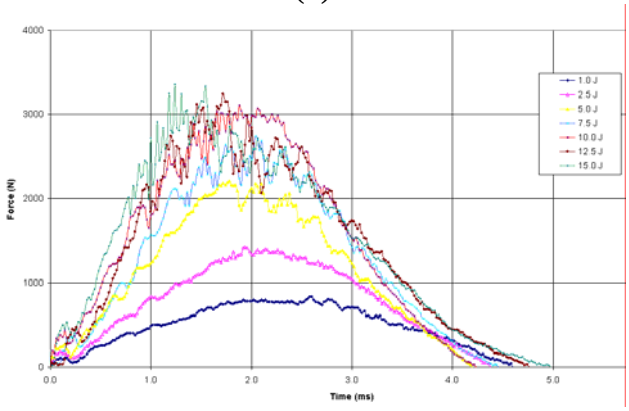

(*b*)

Figure 5: Force-time history for (a) 12.5 mm, and (b) 25.0 mm diameter impactor tups

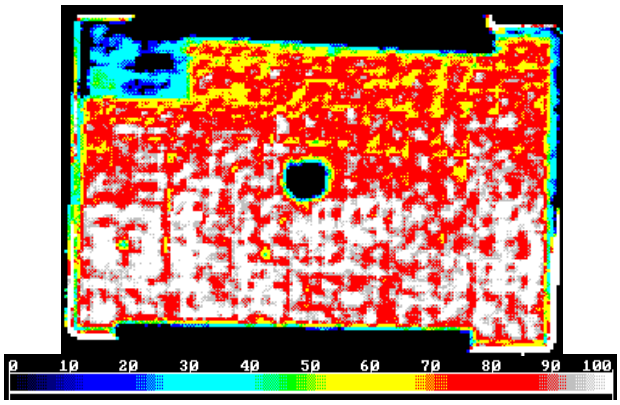

Figure 6: C-Scan for 5.0 J impact energy

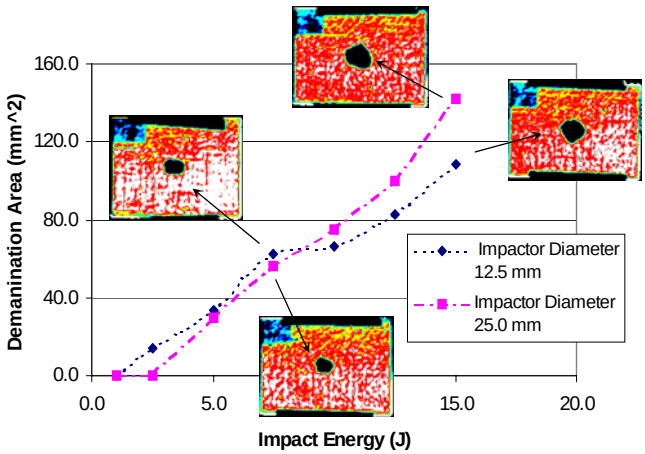

Figure 7: Delamination area versus impact energy

Figure 7 shows that for energies from 1.0 to 10.0 *J*, the 12.5 *mm* tup produced a greater delamination area than the 25.0 *mm* tup. This was due to the larger localised impact force, created by the smaller impactor tup, resulting in a higher deflection of the specimens under the same dynamic loading. However at higher impact energies the smaller tup penetrated the specimen, resulting in the transverse growth of the damage being limited by the tup diameter.

For higher impact velocities, the smaller impactor resulted in significant localised damage that increased the compliance of the laminate within the impact zone. This caused a re-distribution of the loads in this region during the last half of the impact event, hence the second peak in the force-time histories. This is further supported by Figs 8, in which the impact energy versus peak force and indentation are displayed, respectively. It is evident that the 12.5 *mm* impactor created a much deeper permanent indentation in the specimens. The extent of these indentations caused more energy to be absorbed and resulted in an overall reduction of the peak force recorded. The peak forces recorded for the 12.5 *mm* impactor were significantly less than for the larger impactor tup at the same energy.

3.2 FE Modelling

Mesh size

Figure 9 shows the force-time history for one of the tests and that predicted by the simulations with two different mesh sizes. The agreement

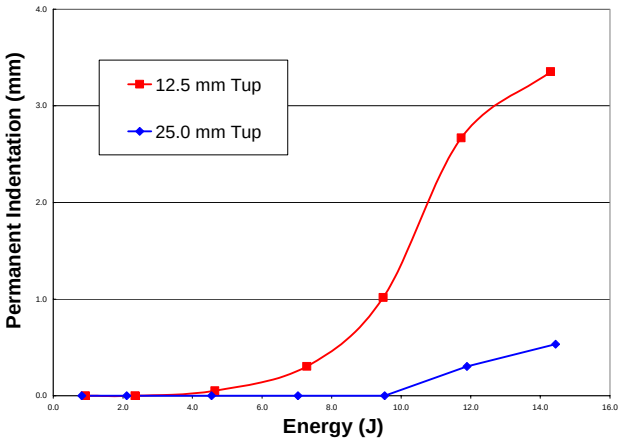

(*a*)

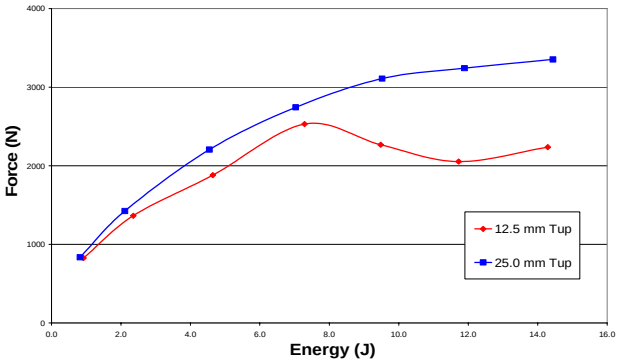

(*b*)

Figure 8: Impact energy versus (a) permanent indentation and (b) peak force

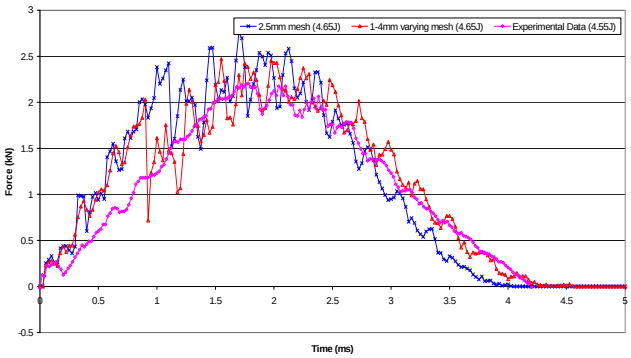

Figure 9: Effect of mesh size on predicted force-time history

between the predicted and test results was better with a 1.0 to 4.0 *mm* variable mesh compared to the constant 2.5 *mm* mesh. Both predictions were less accurate for the loading phase. This was attributed to the idealised boundary conditions, making the analysis unable to account for the initial absorption of the impact force.

It was further established that the damage area predicted by the simulation, using the variable mesh, closely corresponded to that detected by the C-Scans.

Numerical noise, in the form of very high frequency peaks, was observed in most analyses. These peaks were most prominent in the models with coarse elements in the impact region and least prominent in the models with finer elements. This problem was probably caused by the mismatch in element size between the impactor and the panel, leading to problems in surface contact. To overcome this problem it would be necessary to refine the mesh in the impact zone significantly. However, since analysis time was proportional to the minimum element size, this approach would lead to much longer run times. A preliminary investigation of the models was conducted using a refined mesh. The investigation showed that mesh refinement did remove many of the high frequency peaks, but made little difference in the predicted peak force. Therefore the moderate mesh size used in this analysis was considered a satisfactory compromise between accuracy and computation time.

Force-time history

The force-time history for each of the conditions shown in Figs 5 was predicted using Pam-Crash.

Figure 10 shows a typical comparison of the predictions and experimental data. The shape of the force-time plot, peak force and duration of the impact event were predicted with reasonable accuracy. An exception was the 15.0 *J* impact, where the peak force was predicted as much higher than that observed. This difference was attributed to the penetration of the specimen by the impactor at this energy, which was not captured by the elastic solution coupled with the fabric bi-phase degradation module. An element elimination capability would be required in the analysis to account for this penetration. Note that to reduce computational time, the impact window was trimmed, hence the premature termination of the simulation results.

Delamination modelling

Preliminary comparison of the experimental and numerical predictions is shown in Fig. 11. It is evident that the analysis has been able to capture the order of delamination size as well as the directional elongation detected in tested specimens. This study has shown that the

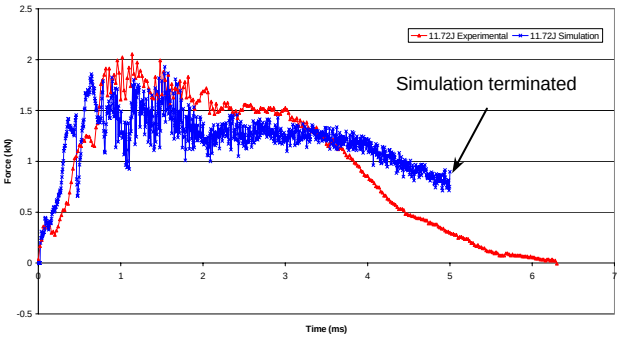

Figure 10: Comparison of experimental and predicted force-time histories for a 11.72 J impact with a 12.7 mm diameter tup

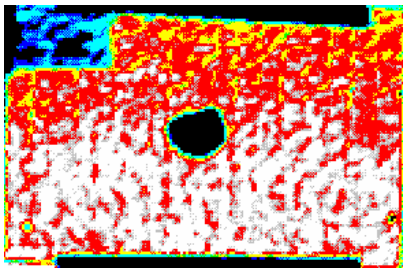

(a)

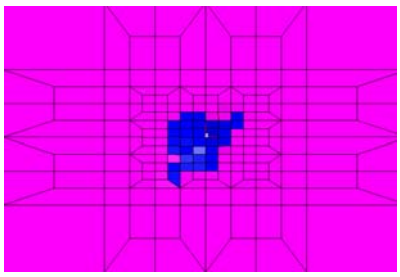

(b)

Figure 11: Comparison between delamination regions resulted from (a) test and (b) simulation under similar impact conditions

numerical approach used, incorporating the fabric composite bi-phase material model and Crisfield delaminations criterion, although somewhat mesh dependent, has a great potential in determining the total area of damage and the delamination region.

Investigations are underway to perfect the modelling methodology, based on the extension of the Crisfield delamination approach, to accurately predict the delamination area. Figure 12 provides an overview of the current stage of the studies aiming at incorporating the delamination effects in the dynamic response of the specimens under low velocity impact loading. A close inspection of the time-force history results indicates that the energy absorbed by the delaminated area within the impact region can significantly reduce the impact peak force, whereas the duration and general response pattern of the specimen stay unaffected.

Future modelling of low velocity impact

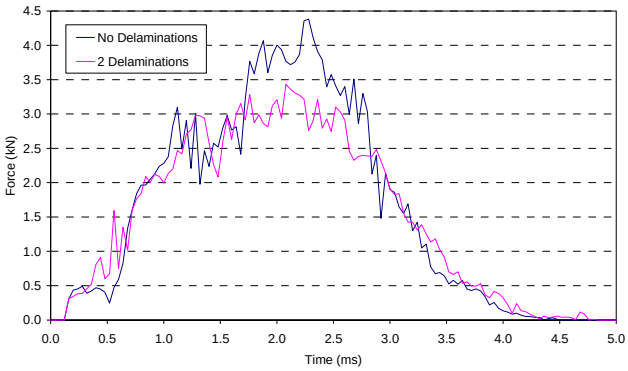

Figure 12: Comparison of force-time response with and without delaminations

in CRPs will focus on refinement of the delamination predictions by including the effects of energy dissipation and permanent out-of-plane deformation. These will contribute to the overall objective of developing a validated, reliable and comprehensive methodology for analysing the complex progressive damage caused by impact. Such a modelling approach may be used in the design and airworthiness certification of advanced composite structures used in aerospace applications.

4. Conclusion

CAI test specimens were manufactured from the same material as that used for a demonstrator CRP (Panel I). Damage was induced in these CAI specimens using an instrumented impact rig and characterised using an ultrasonic C-Scan machine.

FE models of the CAI specimens were created and analysed using the fabric bi-phase composite degradation module, in conjunction with the Crisfield delamination criterion, embedded in the explicit FE code Pam-Crash. There was a good level of agreement observed between the experimental and predicted delamination size and force-time histories for these specimens. It was established that models with a slightly coarser mesh density in the impact zone provided a adequate compromise between accuracy and time.

Application of the impact analysis methodology described in this paper is one step toward demonstrating compliance with the damage tolerance airworthiness requirement for CRPT. This modelling approach also provides a tool with which to improve the impact resistance of future CRP designs.

5. Acknowledgement

The assistance offered throughout this project by Ms D. Allieo and Mr T. Vu in obtaining and analysing the required data and Mr S. McKay in maintaining and supporting the Unix system and the relevant explicit codes, from the School of Aerospace, Mechanical and Manufacturing Engineering of RMIT, is greatly acknowledged. The help provided by Ms T. Perera from the Department of Mechanical Engineering of Monash University in obtaining some numerical results is also appreciated. Special thanks go to Pacific ESI for providing the required FE codes for this project. Aspects of this research work were supported by an Expertise Grant awarded by the Victorian Partnership for Advanced Computing (VPAC). Their continued support of this investigation is highly appreciated.

6. References

[1] Baker, AA, Callus, PJ, Georgiadis, S, Falzon, PJ, Dutton, SE and Leong, KH, *An affordable methodology for replacing metallic aircraft panels with advanced composites*, Composites A, Vol. 35, No. 5, pp 687-696, May 2002.

[2] Harman, A, and Callus, PJ, *Structural analyses of a demonstrator composite replacement panel in a F-111C Cold Proof Load Test*, DSTO-TN-0546, pp 89, March 2004.

[3] Abrate S, *Impact on composite structures*, Cambridge: Cambridge University Press, 1998.

[4] Gdoutos EE, Pilakoutas K and Rodopoulos AC, *Failure analysis of industrial composite materials*, New York: McGraw-Hill, 2000.

[5] Xu, RL and Ares, JR, *Real time damage visualization of composite structures subjected to low speed impact*, Proceedings of ICCM-14. San Diego, CA, USA, 14-18 July 2003: Society of Manufacturing Engineering and The American Society for Composites, 2003.

[6] Mathew FL, Davies GAO, Hitchings D and Scoutis C, *Finite element modelling of composite materials and structures*, London: Woodhead Publishing, 2000.

[7] Bayandor J, Thomson RS, Scott ML, Nguyen MQ and Elder DJ, *Investigation of impact and damage tolerance in advanced aerospace composite structures*, International Journal of Crashworthiness, Vol. 8, No. 3, pp 297-306, 2003.

[8] Kohlgruber D and Kamoulakos A, *Validation of numerical simulation of composite helicopter sub-floor structures under crash loading*, American Helicopter Society, 1998.

[9] Johnson AF, and Pickett AK, *Impact and crash modelling of composite structures: A challenge for damage mechanics*, Stuttgart: DLR, Institute of Structures and Design, 1999.